Validation of a 2D Spinal Cord probabilistic atlas. Application to FA measurement and VBM study of the GM atrophy occurring with age

Manuel Taso[1,2], Arnaud Le Troter[1,2], Michaël Sdika[3], Vladimir S. Fonov[4], Julien Cohen-Adad[5], Maxime Guye[1,2], Jean-Philippe Ranjeva[1,2], and Virginie Callot[1,2]
[1]CRMBM UMR 7339, Aix-Marseille Université, CNRS, Marseille, France, [2]Hopital de la Timone, pôle d'Imagerie Médicale, CEMEREM, AP-HM, Marseille, France, [3]CREATIS UMR 5220 U1044, Université de Lyon, CNRS, INSERM, Lyon, France, [4]Montreal Neurological Institute, McGill University, Montreal, QC, Canada, [5]Institute of Biomedical Engineering, Ecole Polytechnique de Montreal, Montreal, QC, Canada

Target audience: People interested in spinal cord imaging, including post-processing and clinical applications

Introduction: In a recent study, preliminary results about the construction of a 2D multi-slice spinal cord (SC) MR template and probabilistic atlases of the white and gray matter (WM, GM) have been reported (1). Such a template aims at providing a reference and normalized space for group studies and parametric MR analysis or to give an *a priori* knowledge for automated WM/GM segmentation algorithms (2,3).
The purpose of this study was to provide an enriched version of the SC template and to assess its representativity when performing atlas-based automated WM/GM segmentation on new subjects or when analyzing parametric MR images. Its potential use as reference space for Voxel Based Morphometry (VBM) studies was also investigated, by studying GM regional distribution in young and old population and analyzing potential SC GM atrophy occurring with aging.

Materials and methods: ***MR scanning:*** In addition to the 15 young healthy subjects previously included for the construction of the SC atlas (1), 10 new volunteers were recruited for the study (total population 25 subjects, mean age 28±5yo, 9F/16M). Scanning protocol at 3T consisted in a T2*-w multi-echo gradient echo sequence (5 echoes, TE_{eff}=27ms, FOV 180x135 mm^2, resolution 0.5x0.5x5 mm^3, 3 slabs of 7 transverse slices (1 per vertebral level, from C1 to T12) positioned perpendicular to the SC axis, ECG triggering (RR=300ms), T_{acq}~7min/slab). ***Atlas and MR template construction:*** After manual segmentation in three classes (CSF, WM, GM), intensity non-uniformity correction was applied using N3 (4) within the mask of the SC (ie. WM+GM). Inter-slice intensity normalization was performed by normalizing the 90th percentile of the CSF intensity across the different levels for one subject. Atlas and template construction was performed using SC center of mass alignment followed by 4 DOF affine co-registration as described in (1) by using 20 of the 25 subjects, randomly chosen. ***Assessment of atlas-based WM/GM segmentation:*** The 5 remaining subjects were used as test-subjects. Masks obtained from thresholded and binarized SC atlas were registered to the manually defined SC masks of the subject using 5DOF affine registration and FSL linear registration toolkit (FLIRT) (5). SC thresholds from 30 to 70% were investigated (corresponding to 70 to 30% GM threshold respectively). Transformations were then applied to WM/GM masks. Similarity assessments between WM and GM manual ROIs and WM and GM ROIs derived from the thresholded atlas were performed for each threshold, by calculating the DICE and Jaccard coefficients. Statistical differences between thresholds were assessed with a HSD Tukey-Kramer test (JMP9, SAS). ***Parametric MR analyses (FA maps):*** Diffusion tensor imaging (DTI) was performed on 8 new subjects (4F/4M, 30±4yo). Acquisition consisted in a single-shot SE-EPI sequence (TE=75 ms, FOV 128x117 mm^2, resolution 0.9x0.9x5mm^3, 7 slices with one per vertebral level, gap 200%, 30 directions, b=0 and 600 s/mm^2, 4 averages, ECG triggering (RR=300ms), T_{acq}~7min). GM, WM and SC masks were first manually drawn on the FA maps. SC masks were then registered to the SC template. After registration, FA values calculated in atlas-based ROIs were compared to FA values obtained in WM and GM manually delineated. In-ROI STD were also considered. ***VBM study of GM distribution:*** 8 older subjects (3M/5F, 58±6 yo) were scanned at the cervical level using the same T2*-w sequence. The images from C1 to C4 were manually segmented (SC, WM, GM) and the SC was normalized to the template using 5DOF affine registration. Smoothing was performed using SPM8 with a Gaussian smoothing kernel of 1x1x1mm^3 at FWHM (6). Statistical mapping consisted in a two sample t-test between both groups GM masks, with gender entered as confounding variable. $p<0.05$ was set for the significance level.

Results: Examples of probabilistic WM and GM maps are illustrated on *fig. 2*. The SC MR template (C1 to T12) build with n=20 subjects and with intensity normalization is shown on *fig. 1*. The correction/normalization procedure allowed reducing the inter-slice STD in both CSF and SC by 78 and 71% respectively on the MR template (*fig. 3*). *Fig. 4* summarizes the mean DICE coefficients obtained when comparing manual and automated segmentation at different thresholds and combining both WM and GM. On average, values greater than 0.75 were found, except when using the 70/30% threshold, which was significantly lower (DICE=0.659; $p < 0.0001$) and the highest mean DICE was obtained for the 40/60% threshold (=0.808). In WM (data not shown), DICE were all greater than 0.79, and mean DICE for 40/60, 50/50 and 60/40% thresholds were found equal to 0.890, 0.899 and 0.897, respectively.

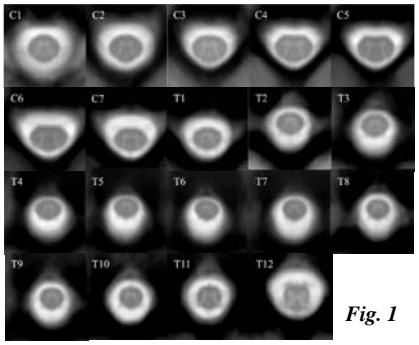

Fig. 1

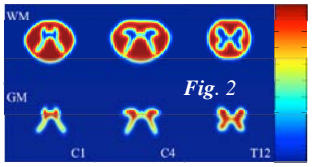

Fig. 2

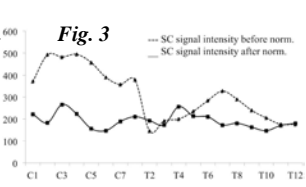

Fig. 3

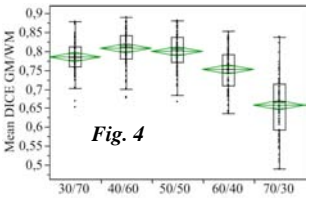

Fig. 4

When using the 40/60% threshold for automated WM/GM FA quantification (*fig. 5,6*), FA in the WM were found similar than with manual segmentation and within the range of previously reported values (7). Both manual and automated segmentation led to significant differences between WM and GM ($p < 0.0001$ and p=0.0001, resp.) and no differences were noticed concerning the in-ROI STD. However in the GM, FA derived from the automated segmentation was higher than that with manual segmentation (0.603 ± 0.062 vs. 0.544 ± 0.061; p=0.0024). This is due to averaging of values in both anterior and posterior GM horns with the automated ROIs, whereas manually segmented ROI rarely considered posterior GM (*fig. 5*). To fully exploit the benefits of an automated segmentation, an erosion of both WM and GM ROIs should thus eventually be performed, in conjunction with a segmentation of WM and GM substructures (lateral/dorsal/ventral, anterior/posterior) (8).

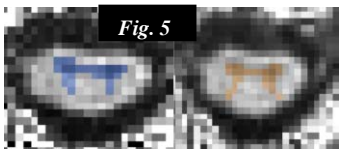
Fig. 5

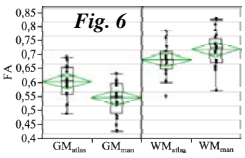

Fig. 6

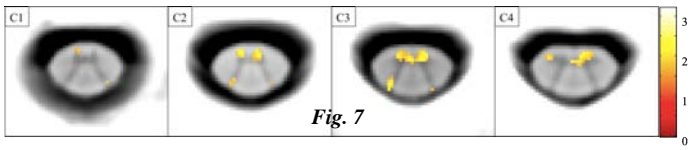

Fig. 7

In complement to a previous study reporting a regional SC atrophy (6), *fig. 7* presents the results of the GM statistical mapping, showing evidence of GM atrophy in the older population when compared to the young population, mainly in the anterior GM horns from C2 to C4 ($p<0.007$), with 2 clusters emerging at C2 (k=11 and 7), one at C3 (k=33) and two at C4 (k=20 and 5), but also some slight evidence of atrophy in the posterior GM at C2 and C3 ($p<0.04$). This neurodegenerative process has been previously reported on *post-mortem* samples (9), and with absolute GM area measurement (10), but its topography is shown here for the first time. Further subject recruitment and examination across the entire SC should of course be conducted to comfort these preliminary results.

Conclusion: We propose here a SC template providing a probabilistic knowledge on the spinal cord WM and GM structures, useful in complement with already existing segmentation algorithms (2,3). In this study, preliminary promising results have been obtained in healthy subjects and potential applications have been presented for parametric MR analysis and voxel-based analysis of the SC structures. Future investigations should now be focused on pathological cohorts.
Further developments should be focused on the integration of a robust automated cord edge delimitation on T2* contrast (11), allowing for a fully automated cord and SC substructures segmentation. Non-linear (NL) registration procedures for registration to the template should also be investigated. Finally, a 3D (interpolated) version of the template is currently under development for enriching current T2/T1-w based template (5,12) lacking of WM/GM contrast. The integrated version aims to be usable in a complete multimodal SC MRI processing pipeline (12) and is part of the MNI_Poly_AMU_v1 SC template.

References: (1)Taso et al, Magn Reson Mater Phy, 2013 (2)Yiannakas et al, Neuroimage, 2012 (3)Ellingson et al, Acad Radiol (2007) (4)Sled et al, Medical Imaging, IEEE Transactions, 1998 (5)Jenkinson et al, Med Image Anal 5, 2001 (6)Valsasina et al, AJNR, 2012 (7) Callot et al, ISMRM 2009 (8)Sdika et al, ISMRM 2010 (9)Terao et al, Acta Neuropathol, 1996 (10)Fradet et al. Spine, 2013 (11)Chen et al, Neuroimage, 2013 (12)Fonov et al, ISMRM 2013